Experimentally optimized and field validated three-dimensional electromagnetic energy harvester for smart farming applications

D. Blažević[*a], J. Ranta[a], M. Grunewald[b], Y. Mizukawa[a],
J. Dizdarević[b], R. Niiranen[c], P. Rasilo[a] and A. Jukan[b]

[a]Electrical Engineering Unit, Tampere University, Korkeakoulunkatu 3, Tampere, Finland; [b]Department of Electrical & Computer Engineering and Physics, Technical University of Braunschweig, Hans-Sommer-Str. 66, Braunschweig, Germany; [c]Ahlmanin koulun Säätiö sr, Hallilantie 24, Tampere, Finland

ABSTRACT

Kinetic energy from vibrations emerging from mechanical systems such as machines and vehicles has been thoroughly studied as a power source in the last two decades. Numerous kinetic energy harvesters have been built to convert human locomotion into electrical power but haven't been implemented on a wide commercial scale. On the other hand, energy harvesters for farm animals haven't been studied as much. In this paper, we present a three-dimensional electromagnetic induction based kinetic energy harvester optimized specifically for cattle wearable applications. All the device parameters are obtained with an empirical optimization procedure by considering specific cattle locomotion characteristics. The prototype is 3-D printed with low friction and impact resistant materials. Finally, the device is tested in a real free grazing scenario with live cattle. The kinetic energy harvester performed well and was able to power the load and transmit animal body temperature data over long distances for up to 7 times/h.

Keywords: Animal locomotion, Energy harvesting, Energy scavenging, Internet of Things, Precision livestock farming, Smart farming, Wearables, Wireless sensor networks

1. INTRODUCTION

Technologies for monitoring animal health, welfare, yield, or other livestock production parameters are usually referred to as precision livestock farming (PLF) or smart farming in a broader sense when considered under the umbrella of the Internet of Things (IoT) [1]. The smart farming technologies used in animal production systems can be either: a) installed on-site like cameras, microphones or climate sensors or b) wearable like animal collars, ear tags, halters or leg straps with embedded sensing and communication devices. These wearable smart farming technologies represent an attractive academic research area due to new data produced and made available to animal and agricultural research communities. On the other hand, they also represent a growing market with millions of devices being sold annually in the EU alone [2]. Although these technologies promise an increase in overall sustainability of animal production systems through better and more precise resource management, animal wearables are mostly powered by finite lifetime batteries and only a small fraction of them employ solar energy harvesting. This practice introduces a hindering effect on the sustainability of the whole system due to pollutive battery manufacturing processes and low rates of battery recycling. Additionally, for these technologies to have high adoption rates, the wearable devices should prove to be energy autonomous to decrease farmers' workloads and decrease or eliminate battery changing and recharging and reduce device downtimes, making these devices resilient in harsh animal husbandry conditions. Even though solar energy harvesting is employed by several companies, most manufacturers choose not to work with solar energy harvesting due to cost, complexity, and unreliability due to high levels of dirt accumulating on the solar panels in farming conditions and poor operation in higher geographical altitudes and indoor systems.

[*] david.blazevic@tuni.fi

Active and Passive Smart Structures and Integrated Systems XVIII, edited by Serife Tol, Guoliang Huang, Xiaopeng Li, Mostafa A. Nouh, Shima Shahab, Jinkyu Yang, Proc. of SPIE Vol. 12946, 129460X · © 2024 SPIE · 0277-786X · doi: 10.1117/12.3010124

To tackle these issues, we envision the widescale adoption of multiple energy harvesting principles in the inception and design of animal wearables for PLF applications. The work presented here details the development of an autonomous smart farming wearable system for cattle with a multi-modal energy harvesting system which uses both kinetic and solar energy in unison. To develop this system a new wearable kinetic energy harvesting (KEH) device had to be built and optimized based on cattle locomotion profiles. A power management system was designed to receive input from both kinetic and solar energy harvesters. Concurrently a benchmark smart farming architecture for measuring animal health parameters was being developed and, in the end, the complete wearable was deployed in the field with live animals. In the following sections we will introduce the recent research in animal wearables and show the empirical procedure leading to the development of the KEH device for cattle. Finally, the details regarding the construction of the proof-of-concept wearable prototype of a smart farming health monitor are shown and experimental results are discussed.

1.1 Animal kinetic energy harvesting and the animal wearables market

Energy harvesting or scavenging is the process of converting low level energy from the environment, such as light, fluid flow, vibration, locomotion, or heat into small amounts of electrical energy by using active materials (i.e. photovoltaic or piezoelectric materials) or a combination of passive components (i.e. magnets and coils). Harvesting energy from the animal body, especially the human body, to power smart electronic wearable devices or medical implants, has been the source of motivation for a large body of energy harvesting research performed in the last two and a half decades [3]. In that sense the human body has been studied extensively, and almost all energy harvesting principles have been applied to the human body with piezoelectric [4], thermoelectric [5], electromagnetic [6], and lately triboelectric energy harvesting [7]. This success has mostly been laboratory based where researchers have been proving constantly over the years that low power electronic devices designed for intermittent measure/transmit/sleep cycles can in fact be powered by some sort of an energy harvesting device. The success can be mostly attributed to advances in low power, and ultra-low power electronics [8] which will in the future facilitate the integration of energy harvesting devices even in greater numbers. Commercially, energy harvesting from the human body has very limited success due to limited performance, reliability, price, and size/weight factor of the energy harvesting devices having a great impact on the choice of electronic device designers to incorporate these techniques into their designs.

a) b) c) d)

Figure 1. The 250-year evolution of an animal wearable: a) The Perrelet self-winding watch back side showing the large oscillating brass weight (cca. 1780)., b) Perrelet self-winding watch front side with one function - displaying correct time, c) Kinetron MGS 32.8 KEH generator, averaging 3-8 J per day, depending on the activity levels, and d) the Sequent Supercharger KEH powered watch (2024). with the Kinetron generator possessing Bluetooth and multiple functions - odometer, heart rate monitor, workout recorder, sleep, and blood oxygen level monitor.

Out of the few successful energy harvesting implementations on the human body we can single out the autonomous wristwatch application – the so-called automatic watch. Here kinetic energy harvesting has seen reliable success and widespread use in modern times since the invention of the watch in 1777 by Abraham-Louis Perrelet, a Swiss watchmaker [9]. In this device the energy harvesting mechanism and energy storage are purely mechanical where the oscillating weight is winding the spiral watch spring during regular wrist movement as shown in Figure 1 [10]. In Perrelet's case the watch was wound for the day if the users, carrying the watch in their pocket, walked regularly for 15 minutes. Modern version of the automatic wristwatch, like the Sequent, couples a small electromagnetic generator, manufactured by Kinetron, in which voltage is induced by the rotor being spun by the oscillating weight as shown in Figure 1 [11]. Thermoelectric watches have also seen moderate success and limited production runs with new designs emerging recently [12]. Other than that, energy harvesting from the human body on a commercial level has been in the

novelty range (like the running LED light) and hasn't been embedded in serious commercial level smart wearables due to limitations of the energy harvesting devices mentioned before. But due to advancements in electronic device energy efficiency, more and more energy harvesting devices will be capable of powering smart wearables as these advancements will allow for reduction in weight and size of the energy harvesters.

On the other hand, non-human animals haven't been studied as intensively in energy harvesting scenarios. The animal wearable weight rule states that the animal wearable shouldn't weigh more than 2-5% of the total animal body weight [13]. Based on this we hypothesize that wearables for large ungulates (cattle, sheep, pigs, and goats) used to carrying heavy loads (i.e. brass cow bells or identification weights) could easily be integrated with KEH generators weighing up to 0.5 kg. A significant trend has emerged in recent years with more and more animals being equipped with wearable smart technologies. From pets and hunting dogs to farm animals and wildlife, animal wearables are becoming a standard for animal safety, control, welfare, and research. As in human wearable or implantable technologies, these smart wearables for non-humans usually consist of a sensor, microcontroller, wireless transmitter, and energy storage (a battery). The sensing function in these devices varies among different applications and among different species [14]. The focus of this work is on technologies for grazing animals and the following overview is based on our own market research and a number of grazing technology reviews emerging in the recent years [15]-[18]. One the most sought-after sensors are Global Navigation Satellite System locators which are used throughout the non-human animal world. These sensors represent a large portion of the existing PLF market for grazing animals where they are used anywhere from theft control, predator determent or finally for behavior control via virtual fencing devices with usage of vibration, sound, or electric shock. These sensors are also commonly used in hunting dog wearables and wildlife trackers. Activity sensors like accelerometers are long established as go-to wearable sensors in PLF used for establishing multiple health and welfare indicators through activity level analysis such as lameness, heat detection and calving, feed intake and overall animal health. Animal body temperature sensing is also one of the common animal health monitoring techniques in PLF (ear or skin-based measurements and inside the rumen). From temperature data the farmer can deduce if a disease is spreading inside the enclosures or if certain individual animal's health is deteriorating. Low level sensors like electronic radio frequency identification tags are used in feed optimization and milking machine identification to track individual animal performance. Usually, the commercially available devices employ several sensing techniques in one device (e.g. identification/acceleration/location are always almost used concurrently).

In order to fully exploit the potential of animal wearable KEH devices, particularly in the context of IoT applications, appropriate communication solutions and technologies, which can ensure energy efficiency and long-range coverage are needed [19]. While a wide variety of technologies is used commercially, according to our analysis the biggest portion of the market, for grazing and non-grazing animals, still relies upon local node and gateway radio networks. In these networks the radio transmitter on the animal sends the message to a locally installed gateway which then communicates to the cloud, as a more resource capable part of the system used for data storage and further processing. Due to the required wide-area coverage for the related applications, traditional short communication range solutions such as WiFi, Bluetooth and ZigBee are no longer sufficient. Solutions based on traditional mobile cellular communications, as well as direct communication via satellite can provide higher transmission coverage, however due to their high energy consumption they cannot satisfy low power consumption requirements of KEH wearable devices. Instead, the focus is on the Low-Power Wide Area Network (LPWAN) technologies, where the three leading technologies include Narrowband Internet of Things (NB-IoT), Sigfox and LoRa [20]. In most of these commercially available devices the battery volume and weight represent more than 90% of the total device volume and weight. Based on the use case, location lock frequency and transmission frequency, these devices can have a lifetime ranging from a few months (like virtual fencing devices) to 10 years (in the most simplified single location lock per day devices). Its noteworthy to say that none of these devices has been on the market long enough to prove the 10-year lifetime. Up until now most of the animal wearables were developed as collars or leg straps (tail and halter as well but much less in quantity). Recently smart ear tag technologies have seen commercial success due to mandatory animal ear tag identification legislation and the miniaturization of PLF wearables where the devices have become sufficiently small and light for an animal to have it attached to the ear. As mentioned before, some companies use solar energy harvesting, like the virtual fencing companies with the largest energy needs (Nofence, Gallagher, Herdwhistle, Halter), but the majority of PLF wearables do not employ energy harvesting.

The number of papers researching energy harvesting from the non-human animal body is limited. Solar harvesting research was performed on zebras [21], north elephant seals [22], tuna [23], pink iguanas [24], turtles [25], and cattle [26]. Some limited research with thermoelectric energy harvesting of sheep has been performed [27]. Considering non-human KEH the largest body of work was performed on piezoelectric harvesting of insect [28], [29] and avian flight [30]

and rodents [31], and implantable KEH in dogs [32], cows, sheep [33] and fish [34]. As far as electromagnetic KEH devices are concerned research has been performed on cattle [35], fish [36] and reindeer [37] together with some purely theoretical studies of electromagnetic KEH for elephants, cattle and other terrestrial wildlife. In 2022 our group published a paper on the study of grazing cattle locomotion as a source of kinetic energy for wearable PLF devices [38] and a field trial of a cattle optimized 1-D leg strap based KEH with an embedded Bluetooth beacon [39]. In the most recent study from 2023 a team of researchers built a kinetically powered GPS/Sigfox wearable for wildlife where for KEH they employed the off-the-shelf Kinetron MGS 32.8 electromagnetic energy harvester [40]. The study was performed on dogs, bison, and a pony. A pony fitted with a 'Kinefox' collar was able to power a GPS location and Sigfox transmission every four days in an experiment lasting 6 months. The study mentions several issues concerning the sturdiness of the moving parts of the Kinetron harvester, especially the magnet ring which broke several times.

2. 3-D ELECTROMAGNETIC KEH DEVICE DEVELOPMENT AND OPTIMIZATION

To extract the largest amount of energy, inertial KEH devices must be optimized so that their first fundamental resonant frequency corresponds to the steady-state excitation frequency of the host structure, i.e., the device, structure, or body they are attached to. If this is the case, the displacement of the moving parts can reach the largest amplitudes or speeds, resulting in the largest amount of energy harvested from the host structure. In human or non-human energy harvesting there are two underlying characteristics of motion that undermine the resonance frequency tuning for achieving maximum harvesting efficiency: a) animal locomotion is inherently stochastic and infrequent due to large amounts of idling and b) the characteristic frequencies of the animal bodies are found in the range of 1-10 Hz, inherently increasing the size and weight of moving KEH device parts if they are to be coupled to such low excitation frequencies. Although bandwidth broadening strategies for increasing KEH device frequency of operation do exist and were proven successful in the laboratory, this usually implies increased complexity of devices [41]. For KEH from the animal body, the electromagnetic (EM) KEH devices have proven to be most successful. A commonly researched scenario of an EM KEH device is shown in Figure 2 a) where a moving magnet placed centrally in a cylindrical tube is inertially excited by base excitation $y(t)$ and is allowed to move inside the tube resulting in relative motion $z(t)$ which in turn induces voltage in the copper coil wrapped around the tube. The axial movement of the moving magnet is restricted by magnets of opposing polarity on each side of the tube which act as magnetic springs with magnetic force F_m and define the resonant behavior of the system. The circuit diagram on the right of the tube shows the EM KEH generator as an AC voltage source in series with the coil resistance R_c and inductance L and an equivalent load resistance R_l.

The most common types of electromagnetic (EM) KEH devices can be summarized according to three approaches to establish the motion of the moving part (mostly magnets): translation, rotation or rolling motion. Translational devices include all types of devices in which the moving element has a predefined orientation and can move in one or two dimensions without changing the orientation. These can include 1-D tubular devices, 2-D sliding or circular motion and cantilever-based devices. Rotational devices also have a predefined orientation of the polarity of the moving parts and can be divided into two architectures: a) direct coupling architecture in which the moving element of the KEH generator, the rotor, is coupled directly to the source of rotation (shaft or rotating joint) and b) gravitational architecture in which the rotor of the KEH generator is coupled with a pendulum weight which is displaced inertially by the movement of the host structure. Finally, there are rolling KEH devices where the moving magnet doesn't have a predefined orientation and is able to roll in one, two or three dimensions based on the design of the rolling surface (tube, plane or sphere).

2.1 Spherical KEH: architecture and design of experiment

A basic design of a spherical KEH device is shown in Figure 2 b) where the important dimensional parameters are identified as the spherical cavity diameter D_S, the diameter of the moving ball magnet (MBM) D_M and the minimum inner diameter of the coil D_C. Figure 2 c) displays the intended location of the wearable KEH generator. A similar design has been previously reported and optimized according to parameters such as number of coil turns, coil orientation (latitudinal or longitudinal), cavity volume, and the ball-to-cavity ratio [42]. In this architecture the MBM is specifically designed to move freely, constrained only by the wall of the cavity, and can be inertially excited in 3-D with the downside being the random polarity of the MBM. As the KEH device is inertially excited by the host body, the MBM reacts and rolls or slides across the wall of the spherical cavity towards the cavity edge. As the host body restores balance, the ball travels back towards the center of the cavity and oscillates until stopping or until another excitation occurs. While moving, the MBM has the highest speed at the bottom of the cavity and that's the best possible position for a pickup coil due to the biggest change of the time varying magnetic field. The device cannot be optimized according

to magnet polarity like in purely translational KEH designs although some research has tried to overcome this issue by means of a tethering magnet [43]. Previously reported harvesters had small cavity diameters and were thus optimized for higher frequency excitations. This work is based on the premise that spherical EM KEH devices are especially well suited for cattle collar-based wearables. Based on our previous experience with cattle wearables and insight into cattle locomotion profiles, we have developed an empirical KEH optimization framework in which we optimized for MBM diameter D_M, cavity diameter D_S, coil diameter D_C and number of coil turns N. The empirical design process was greatly facilitated by using the precise stereolithography 3-D printer Form 3 by Formlabs Inc. which was used to print all the specific spherical cavity and coil former designs.

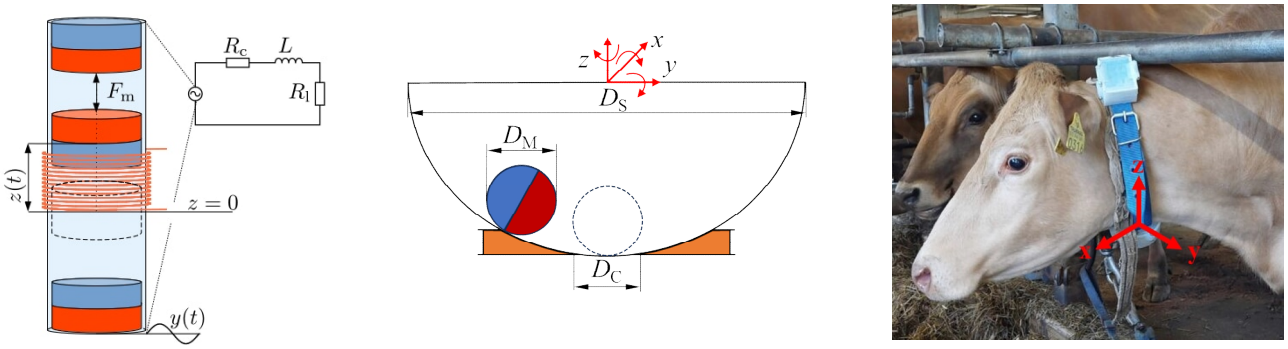

a) b) c)

Figure 2, a) 1-D electromagnetic induction KEH device and circuit diagram, b) schematic of a spherical KEH device indicating optimizable parameters and c) the coordinate systems marks the intended location of the wearable KEH generator

2.2 Coil design and empirical optimization procedure

Coil size and position are significant parameters which determine the efficiency of the EM coupling of the MBM magnetic field to the coil. Table 1 summarizes the design of the experiment with the goal of finding the optimal coil diameter D_C in which the MBM diameter D_M was chosen as the leading parameter due to off-the-shelf availability of certain MBM diameters. For each MBM diameter, three cavity diameters D_S were chosen from the perspective of KEH wearable practical size and volume. Initially 50, 100, and 150 mm cavity diameters were chosen as starting dimensions but the 150 mm cavity soon proved to be impractical. The diameter of 118 mm was added after the analysis described in Section 2.3 and will be discussed later. For each cavity diameter, several possible practically feasible coil diameters were designed with respect to the cavity diameter**.** The spherical cavities were 3-D printed with Durable resin (FLDUCL02) having a uniform wall thickness of 2 mm and with rectangular protrusions on the bottom which allow for precise mounting and quick exchange of different coil formers (Figure 3 a). These coil formers were subsequently 3-D printed as separate parts so that they are as close as possible to the MBM rolling surface and with bottom holes which allows them to be easily attached to the bottom part of the cavity (Figure 3 b). The pickup coil itself was manually wound with enameled copper wire with a diameter of 0.1 mm on a customized QIPANG FZ-180 coil winding machine and a total of N = 1000 turns which is a number chosen to facilitate coil manufacturing while enabling sufficient voltages to be induced in the coil.

Table 1. Design of experiment for coil diameter and position. The 50 mm cavity could only accommodate smaller coils while in the case of the 118 mm cavity, smaller coils behaved didn't induce enough voltage and were thus removed from the experiment.

D_S (mm)	D_M (mm)	Magnet grade	D_C (mm)					
50	19	N38	17	30	37.5			
	26	N38	17	30	37.5			
	30	N40	17	30	37.5			
100	19	N38	14	30	45	55	65	75
	26	N38	14	30	45	55	65	75
	30	N40	14	30	45	55	65	75
118	19	N38	30	50	65	75		
	26	N38	30	50	65	75		
	30	N40	30	50	65	75		

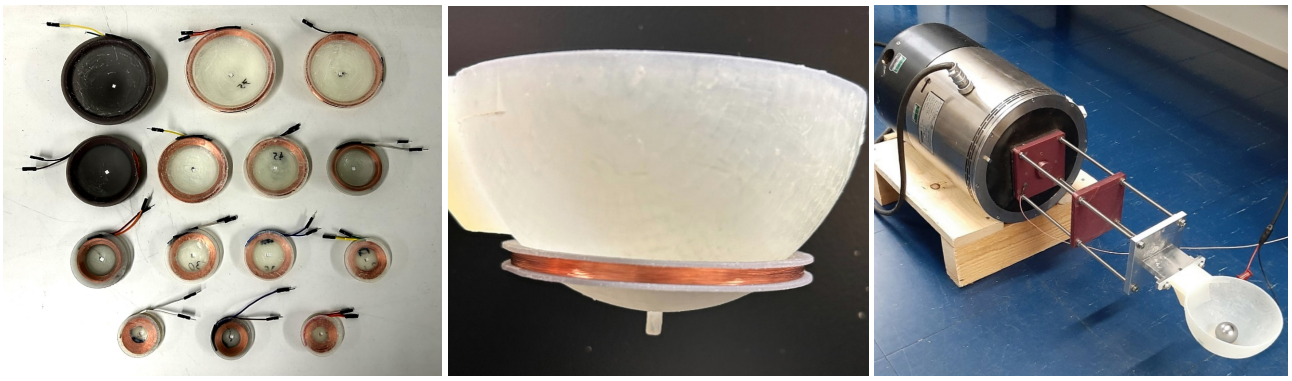

a) b) c)

Figure 3. a) A variety of manufactured coils, b) coil attached to the bottom spherical cavity by a guiding protrusion, c) horizontal laboratory shaker set-up for determining the dynamics behavior of the harvester with different coils, MBMs and spherical cavities all used according to the design of the experiment

A dynamic experimental set-up was designed to test these coil and cavity designs and the harvester, by using the horizontally mounted Brüel & Kjær laboratory shaker with 4805 body and 4813 shaker head (Figure 3 c). The harvester was mounted at the far end of the shaker with a set of long non-magnetic threaded rods, an aluminum attachment interface, and non-magnetic screws. In this way the harvester was kept away from the shaker body to avoid the influence of the magnet inside the shaker on the MBM and the coil. To control the shaker and measure the harvester's response, a National Instruments USB-6251 data acquisition (DAQ) device was used. A frequency modulated sine wave was output via the DAQ to a Venable 1000 amplifier which was then used to drive the shaker. The frequency modulated sine wave has a 0.20 Hz baseband signal which is modulated to carry 2-5 Hz deviation to emulate specific frequencies associated with our previously measured and analyzed cattle locomotion data [38]. The open-circuit voltage is hence acquired at a sampling frequency of 10 kHz for three consecutive minutes for each configuration specified in the design of the experiment as seen in Table 1. To evaluate all the experimental configurations, absolute values of the open circuit voltages are averaged for each coil used and their values are compared as shown in the voltage graphs in Figure 4. On all three graphs it can be seen that larger MBMs eventually induce larger voltages due to stronger remanent magnetic flux.

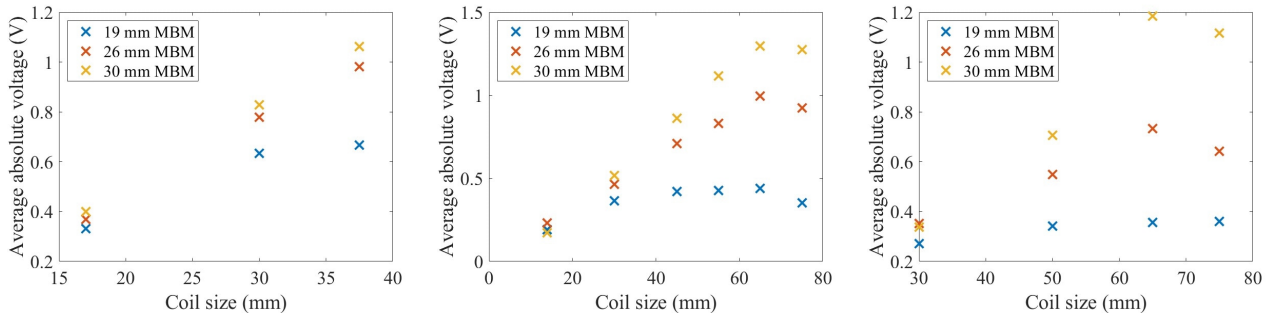

a) b) c)

Figure 4. Coil size optimization experiment for: a) D_S = 50 mm, b) D_S = 100 mm and c) D_S = 118 mm

Generally, the lowest induced voltages occur when the smallest coil diameters are used. This effect is due to the voltage being induced by the MBM in the same direction at the opposite sides of the coil thus resulting in voltage cancellation effects. As the diameter of the coil increases so do the induced voltages and the cancellation effects diminish because the MBM's magnetic field doesn't reach both sides of the coil at effectively the same time. For both the 100 and 118 mm cavity diameters, the peak recorded voltages and the optimal coil diameter D_C are found at approximately 65 mm coils (Figure 4 b and c), while for the 19 mm magnet the optimal coil diameter is found somewhere in the region of 55 mm (Figure 4 a). At the smallest cavity diameter of 50 mm, it wasn't possible to compare with coils larger than 37.5 mm since they practically cannot fit at that cavity diameter. Resulting from these measurements two useful ratios are established which can be used to further analyze the results and deduce which is the most important factor in this optimization problem: the cavity-to-coil diameter ratio and the MBM-to-coil diameter ratio. The cavity-to-coil diameter ratio doesn't have a large effect on the voltage induction while the effect is more pronounced when observing the MBM-to-coil diameter ratio which is slightly different for all three MBMs but can be approximated as 0.4 (Figure 5 a). The

influence of different numbers of coil turns was also investigated. For the spherical cavity D_S = 118 mm, three different coils with inner diameters of D_C = 65 mm were wound with N = 1000, 3000 and 5000 turns and tested with the same aforementioned experimental procedure. In Figure 5 c) it can be seen that, although according to Faraday's law the relation between the voltage and number of turns in the coil should be linear, in the case of spherical KEH devices the relationship is slightly non-linear (as previously investigated in [42]) and reaches a certain saturation threshold. The reason for this may be in the outer coil turns being far away from the MBM. The number of turns should be set to a value which corresponds to the appropriate voltage input levels of the downstream load electronics.

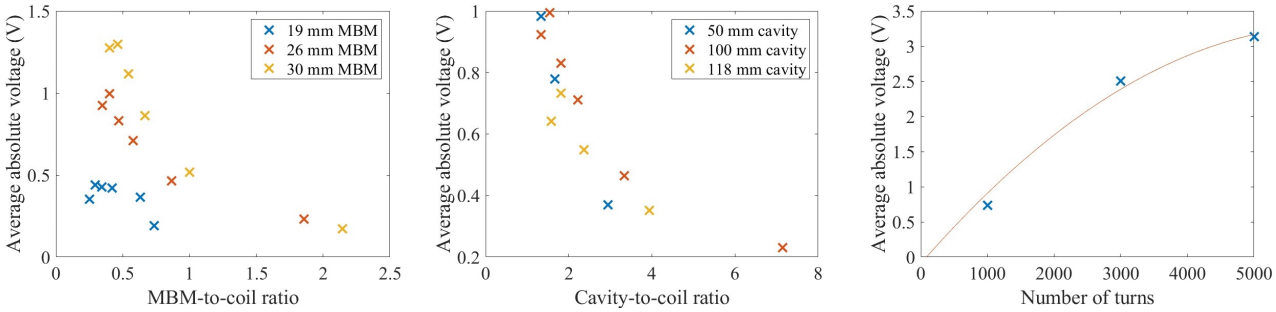

a) b) c)

Figure 5. a) MBM-to-coil ratio for three different MBM sizes, b) the cavity-to-coil ratio for the different cavity diameters, c) influence of the number of coil turns on the induced voltage for the cavity diameter of 118 mm

2.3 Optimal MBM size and cavity diameter analysis

In general, the volume of the harvester is determined by its cavity diameter while the weight is determined by the MBM and coil size. The MBM and the coil are made of metal (neodymium-iron-boron magnets and copper wire) as opposed to polymers used to construct the cavity and thus contribute to most of the weight. Larger magnets have larger magnetic flux so with larger magnets it's easier to induce larger voltages in a coil of the same size. By considering the spherical KEH device as a classic pendulum problem, we could easily define the resonant frequency of the system by defining the length of the pendulum L: from the pendulum pivot point in the center of the sphere to the center of the MBM as shown by Figure 6 a). As mentioned above by matching the resonant frequency of the KEH device its performance could be significantly increased even in the case of animal locomotion without steady-state oscillation. The pendulum analogy provides an extremely simplified way to obtain fast values for an optimal cavity diameter. The basic equation which defines the pendulum's undamped period of oscillation can thus be defined as

$$T = 2\pi\sqrt{\frac{L}{g}} \tag{1}$$

where T is the undamped pendulum period, L is the pendulum's length and g = 9.81 m/s^2 is the gravitational acceleration. However, in the case of a freely oscillating system in the real world damping must be considered. In our KEH device, damping occurs due to surface roughness, electric resistance, and air resistance. Damping can be expressed by introducing the damping ratio ζ to calculate the damped period of an oscillator [44] as

$$T_d = \frac{2\pi}{\sqrt{1-\zeta^2}}\sqrt{\frac{L}{g}}. \tag{2}$$

This equation will be used to compare the theoretical pendulum period values to the spherical KEH prototypes in a series of experiments which are performed by dropping the MBM from the top edge of the cavity – which in our case is the approximate maximum amplitude to be achieved in practice. Before each drop, the polarization direction of the MBM is set to be perpendicular to the cavity's z axis thus setting a uniform initial condition for each drop test (Figure 6 b). The MBM is then allowed to freely oscillate inside the cavity until stopping while the open circuit voltage from the pickup coil is measured and recorded by employing the measurement devices described in Section 2.2. Figure 6 c) shows a typical voltage waveform from a drop test obtained by dropping a 26 mm MBM in a 100 mm diameter cavity with a coil diameter of 30 mm. The magnet's polarization changes quickly and constantly after the first period of oscillation and thus influences the amplitude of induced voltage greatly, resulting in a non-linear damped waveform. As seen in the

waveform, the amplitude can rise due to suitable MBM polarization orientation even though the past period was lower in amplitude. The damping of the MBM comes from a unified influence of friction due to the surface roughness of the cavity, air resistance and magnetic damping.

a) b) c)

Figure 6. a) The simplified pendulum schematic showing the calculated length of the pendulum *L*, b) image of the conducted drop experiment where the magnet is aligned on the edge before each drop, c) recorded induced voltage waveform

Because of the changing polarization and damping of the MBM, only the first period of the waveform is taken into consideration and used to estimate the first damped oscillating periods of the pendulum. Five individual drop tests were performed for the cavity diameter of 100 mm, and averages of the frequencies obtained by measuring the first oscillation periods in the waveform are displayed in Table 2. By utilizing Equation (2) the damping ratio ζ can now be obtained as

$$\zeta = \sqrt{1 - \frac{4\pi^2 L}{T_d^2 g}} \tag{3}$$

by inserting the measured periods. The squared value of the ratio ζ was estimated from the experimental results with the cavity diameter of 100 mm to be approximately $\zeta^2 \approx 0.3291$. By utilizing Equation (3) and inserting the calculated damping ratio, we can now calculate the pendulum length L for a certain target frequency ω_d as

$$L = \frac{g(1-\zeta^2)}{\omega_d^2} \tag{4}$$

By referring to our previously analyzed animal locomotion data and targeting the cattle locomotion frequency measured at ~2 Hz, we can obtain the optimal value for the spherical cavity diameter D_S = 118 mm for the 26 mm MBM and D_S = 123 mm for the 30 mm MBM. The bottom part of Table 2. shows the measured data from experiments including the subsequently built spherical cavity with a diameter of 118 mm matching the desired ~2 Hz cattle locomotion frequency.

Table 2. Calculated pendulum lengths and measured first damped period frequencies for two cavity diameters

	D_S = 100 mm				**D_S = 118 mm**		
MBM diameter (mm)	19	26	30		19	26	30
***L* (mm)**	40.5	37	35		50	46.5	44.5
f_{av} (Hz)	2.2	2.25	2.3		1.92	1.96	2.04

3. DEVELOPMENT OF A BENCHMARK SMART FARMING SYSTEM

To validate the developed KEH device in a realistic smart farming scenario, a complete benchmarking PLF system was developed consisting of a KEH powered cattle collar designed to measure the animal's body temperature and transmit the data with long range radio (LoRa), and a gateway LoRa receiver and transmission logging device installed onsite at the experimental farm (Ahlman dairy farm, Tampere, Finland). Additionally, the collar was equipped with a flexible solar panel produced by Jiang rated at 0.3 W and 1.5 V (200×30 mm^2) to test the multi-modal power generation scenario which showed that the photovoltaic and kinetic energy harvesting can work in unison.

3.1 Power management in a KEH wearable system

Stochastic power output from a KEH device must be controlled to make it utilizable for a microcontroller load [45]. In animal locomotion based KEH scenarios the energy output is stochastic and usually found in a certain range of amplitudes and frequencies. Harvested energy must be stored over time in an energy buffer to gather enough energy for the load to run at least one full cycle of operation. One cycle of operation in a conventional IoT system usually consists of three separate tasks: start-up (or wake-up if in sleep), measurement, and data transmission. After enough charge is collected and the load has run one full cycle, the system can either continue operation or be shut down to wait for enough energy to be harvested for another cycle. In continuous operation, the system is put to sleep for a certain amount of time before running the next cycle. Continuous operation would require continuous excitation from the host body or a sufficiently large energy buffer, i.e., a battery, which would allow it to work when the excitation is not present. In the benchmark smart farming system presented in this work, it is more energy efficient to shut down the power supply to the load after one cycle and run a second cycle after enough charge is collected again. This also facilitates estimating the total energy produced by the KEH device.

In this wearable, the KEH device is an alternating current (AC) source, and the solar panel is a direct current source (DC). The designed power management system must be able to condition both efficiently, and they must be able to work together in unison. The power management for the KEH device must be able to handle a wide range of voltage inputs without too high losses. The whole system must also fulfill the load input requirements defined by the selected microcontroller unit. From a variety of commercially available power management integrated circuits (PMICs), we chose Linear Technology's LTC3588 [46] for the KEH device and Analog Devices' ADP5092 [47] for the solar panel. The LTC3588 has an in-built diode bridge rectifier to rectify the AC input to which the KEH device is attached. The input energy is stored in a buffer, usually a capacitor. These two PMICs charge a shared energy buffer, and the energy output is supplied from the LTC3588. Output is regulated to 3.3 V with an internal buck converter in the LTC3588 to satisfy downstream load requirements (Figure 7).

Batteries, supercapacitors, and conventional capacitors can be used as an energy buffer in KEH systems. It was calculated and measured that a regular capacitor can store enough energy for functional operation for the presented benchmark case. The buffer is first charged to the upper voltage threshold set internally by LTC3588, after which the electrical energy can be transferred to the load. After the storage element voltage falls below an internally set lower voltage threshold, the energy output from the PMIC ceases. The amount of energy transferred from the capacitor and the required capacity of the storage capacitor can be calculated by utilizing Equation (5) [46] as

$$E = \frac{1}{2} C (U_{\text{upper}}^2 - U_{\text{lower}}^2) . \tag{5}$$

In Equation (5), U_{upper} is the upper threshold voltage, U_{lower} is the lower threshold voltage, C is the capacitance of the storage element capacitor, and E is the output energy. The voltage threshold values can be set from four different internal values in the LTC3588. The selected upper threshold voltage is 5.05 V, and the lower threshold voltage is 3.67 V.

3.2 Data management and wireless communication

The system in this work is designed as a complete PLF wearable benchmark system which takes a skin temperature measurement from a cow's body and transmits it wirelessly. For the design and development of this wearable device with a KEH power source as our IoT node, we use a sensing component, a low-power microcontroller unit (MCU) to sample the data from the sensor, and LoRa radio modules for the remote communication with the edge or cloud computing gateways. In this manner, the device is assumed to act as a sensor data generator, sending the data to a gateway device with LoRa protocol, and ensuring a full IoT-edge/cloud computing system integration. Among the previously mentioned LPWAN energy efficient and long-range wireless communication solutions, we opted for LoRa, as it is often preferred choice for smart agriculture applications. Moreover, LoRa can be used in a design of an open-source gateway [1], within a simple integration with widely popular IoT application layer protocols such as MQTT [48], eliminating the need for proprietary and costly solutions. In this work, one wireless node (the wearable) and a single gateway emulate a miniature IoT network. The gateway wasn't connected to the Internet in this scenario.

[1] https://github.com/Jasenka11/IoT-continuum

To meet the requirements of reliable and low-power electronics, the DS18B20 temperature sensor [49], Adafruit Feather M0 Adalogger MCU [50], and RFM9x radio module [51] are selected. The same MCU and radio module are used in the gateway device as well. Additionally, the gateway features a DS3231 real-time clock [52] to track the correct timings of the signal transmissions, and a microSD memory card is attached to MCU card port which was then used to log the received data. Acceleration is also measured with a separate circuit in the last experiment to investigate the influence and coupling of different acceleration directions and amplitudes on the output voltage of the KEH device. The acceleration measurement setup is powered by a battery to run continuous measurements and avoid interference with the KEH system. A MMA8451 accelerometer [53] is selected for these experiments. Schematics of the complete system are presented in Figure 7.

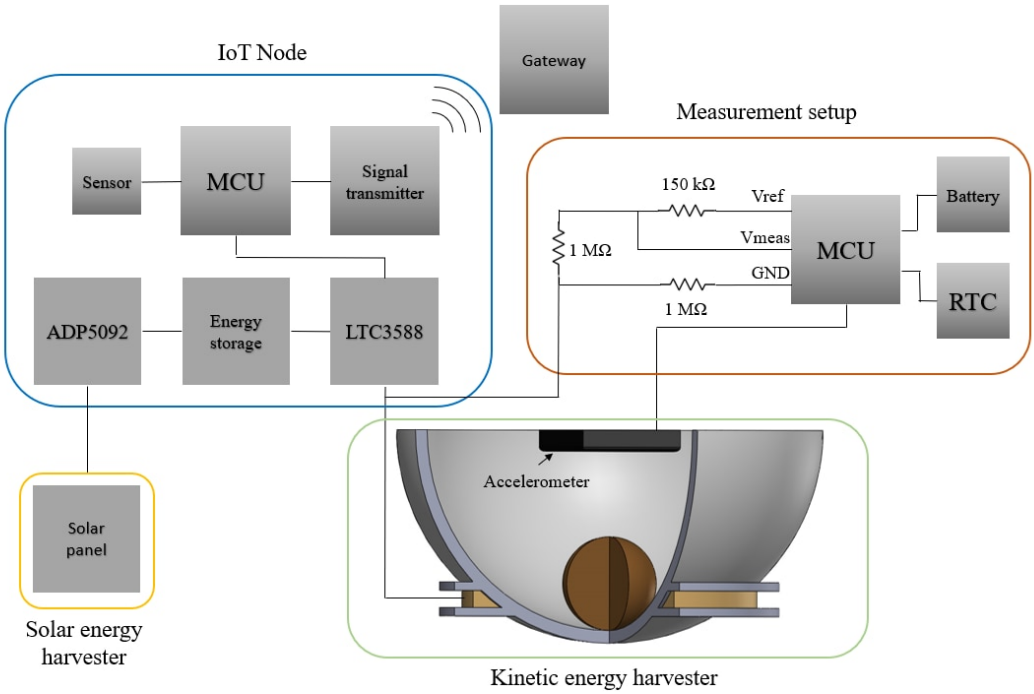

Figure 7. Schematics of the precision livestock farming wearable system built to benchmark the KEH device

After the MCU has initialized, a temperature sample is measured, and the data is sent wirelessly to the gateway with the radio module. After one cycle the MCU shuts down unless there is excess energy due to active excitation from the host body. In this case, the MCU could be able to run an additional cycle of the program without shutting down. LoRa by Semtech, was chosen as a suitable communication technology for this system due to its low energy requirements, long range of transmission and because it is commonly used in smart farming solutions. Since the energy for powering the IoT KEH device was expected to be very low, the LoRa transmission parameters, including bandwidth, spreading factor and coding rate had to be optimized. These values were chosen as 125 kHz, 7 and 4/5, respectively. On the gateway side, the 433 MHz unlicensed frequency band is used with a straight monopole whip antenna while a quarter wavelength conductor antenna is used in the wearable. The gateway setup can be seen in Figure 8. The RFM9x signal transmitter supports signal strengths of 5-23 dBm. A signal strength of 9 dBm was found to be strong enough in the target environment (for up to 1 km of target distance).

An accelerometer is used to measure acceleration from the KEH cavity case to evaluate the effect of acceleration on the output voltage, and to verify the frequency matching with the KEH device. A separate MCU with a battery is used to run continuous acceleration and energy harvester output voltage measurement concurrently. The same MCU as in the wearable is used in this subsystem. As the output voltage levels from the KEH device are too high for MCU measurements, a voltage divider is used, which can be seen in Figure 7. Another DS3231 real-time clock is used to enter correct log times.

All the electronic devices are assembled on prototyping boards, which can be seen in Figure 8. The prototype board is designed to physically fit the wearable, and it is optimized for minimal power consumption. To minimize power consumption, the settings for the signal transmission have had to be optimized. The signal strength is set to 9 dBm, which is the lowest possible value while retaining reliable operation. The sent message contains a string consisting of the experiment name, temperature data, Received Signal Strength Indicator (RSSI) and the number of the sent signals while being powered on. The number of sent signals is used to accurately measure the utilized KEH power. This message can be sent in as low as 3 B to minimize the signal length and thereby lower the signal transmission power consumption. While transmitting the original unoptimized message, the signal transmission consumed 9.9 mJ and this set-up was used in the first set of experiments. By lowering the size of the message length to 3 B, the total energy consumption of the signal transmission was reduced to 4 mJ and this was then the set-up employed in the last field experiment. The total energy consumption of one cycle with the unoptimized message was measured to be around E = 45 mJ. Utilizing Equation (5), a 7500 µF capacitor was calculated to store enough energy for the MCU to run one full cycle. Considering potential losses, a 10000 µF capacitor was selected from off-the-shelf components for reliable operation of the system.

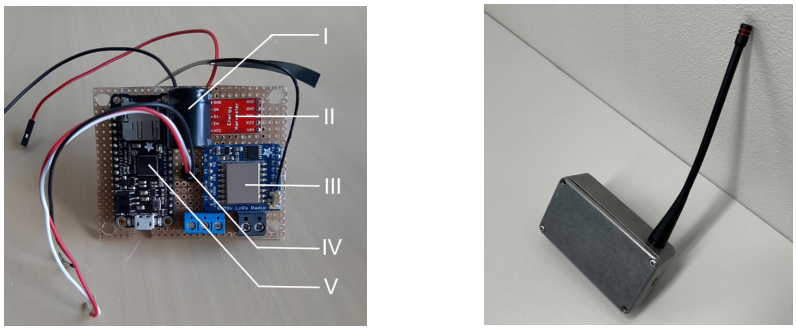

a) b)

Figure 8. a) The prototype board: I) energy storage, II) PMIC, III) radio module, IV) temperature sensor, V) MCU, and b) the assembled gateway comprising of an identical MCU and communication unit as in the wearable

3.3 Development of a benchmark PLF system prototype

Two KEH devices are built for the experiments:

a) Version 1 - optimized for size with: D_S = 118 mm and D_M = 26 mm, and

b) Version 2 - optimized for performance with: D_S = 123 mm and D_M = 30 mm.

Coils with D_C = 65 mm are used as they proved to be the most efficient for these cavities in laboratory experiments. The coils are manually wound to have 5000 turns to ensure high enough voltage for the PMIC, which has a wake-up voltage threshold of 3.3 V.

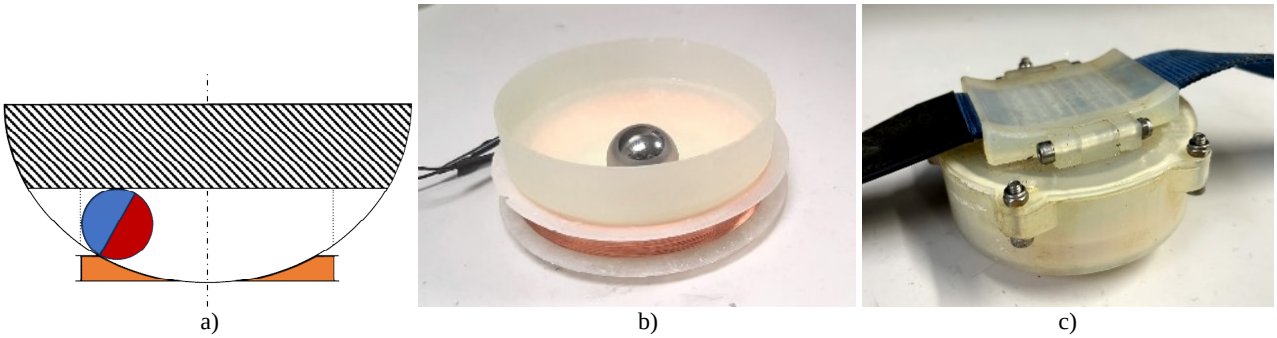

a) b) c)

Figure 9. a) 2-D schematic of the cavity showing the cavity cut-off region which was then removed from the design to reduce device volume, b) image of the Version 1 3-D printed KEH prototype with the wound optimized coil, c) the fully assembled KEH device with the spherical cavity, MBM and the coil secured inside an outer casing

For a wearable device, the volume of the KEH device should be optimized to be as low as possible. The MBM rarely achieves maximum amplitude, i.e. the top part of the spherical cavity. In this position it is the furthest away from the coil hence the induced voltage levels will be low. To make the device more compact it was decided to utilize only a portion of the spherical cavity, as expressed in Figure 9 a). The height of the KEH device is cut to the point where the center of the MBM will still be able to reach the center of the coil. The corners where the magnet cannot reach anymore are also cut off. The remaining height of the Version 1 KEH device will be 41 mm and the sphere volume will become 290 cm^3 (as opposed to 475 cm^3). The final prototype of the Version 1 sphere can be seen in Figure 9 b).

The KEH device must be enclosed, and the coil and the wiring require protection. It must also be attached to the collar. A cover is built by 3-D printing the collar attachment and the protective case by using the same Durable (FLDUCL02) impact resistant resin by Formlabs. The cover consists of three different parts, which are attached together with stainless steel screws to minimize interaction between the MBM and the screws. The final encased Version 1 device is displayed in Figure 9 c). A slightly larger cover had to be built for Version 2 KEH device.

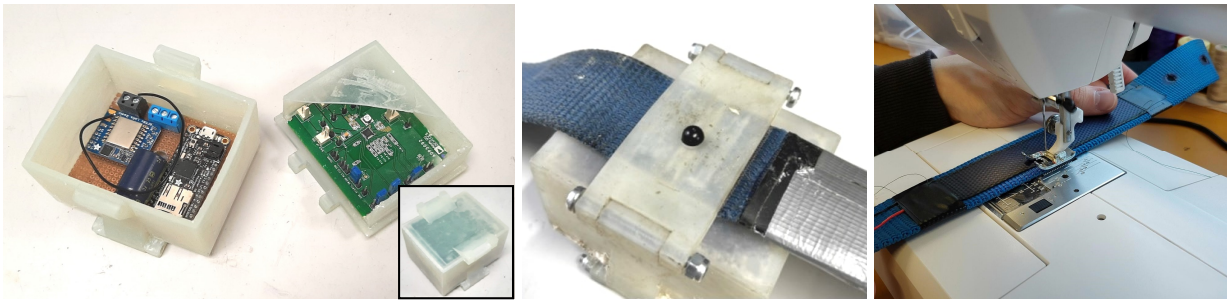

a) b) c)

Figure 10. a) The electronics box showing the arrangement of two separate PMICs while open and closed, b) the bottom of the electronics box showing the digital temperature sensor probe protruding through the box and the collar to allow skin contact with the cow's neck, and c) the procedure of sewing the solar panel into the collar with synthetic thread.

The electronics of the system have had to be protected as well. There are three different circuit boards, one for the MCU and the PMIC, one for the photovoltaic PMIC, and one for the acceleration measurement setup. They are placed inside a 3-D printed protective case. Two of the used boards will fit in the box at once, as only two of them will be used simultaneously (either the MCU and PMIC with the photovoltaic PMIC or the MCU and PMIC with the accelerometer set-up). The box, shown in Figure 10 a), is designed for ease of replacement of the electronic boards and protection from impacts, dirt, and water (by means of silicone-based sealant). Placement of the temperature sensor is crucial, as it should always be touching the cow's skin for accurate measurements. The temperature sensor is put through the bottom of the case (Figure 10 b) and the case is placed at the top of the collar, i.e. top of the cow's neck. In this way, the greater weight of the KEH device below the cow's head is anchoring the sensor in the correct position during the measurements. The lead wires connecting the KEH device and the electronics box are protected with insulation tubing as they run through it across the collar. The flexible solar panel is sewn on the collar next to the electronics box (Figure 10 c). The solar panel also covers the wiring, as leads go underneath it. The final prototype can be seen in Figure 11.

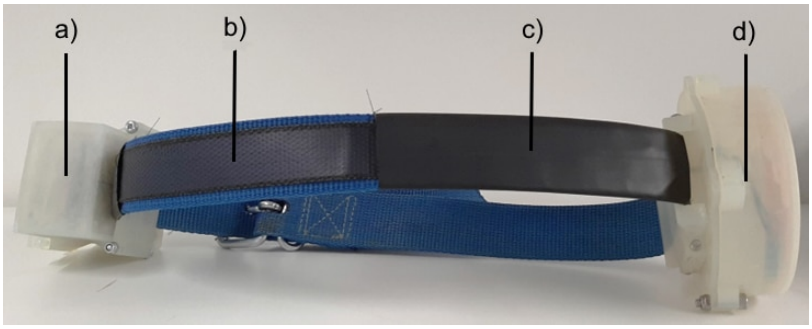

Figure 11. The fully assembled prototype collar device used in field experiments with cattle consisting of: a) the electronics box, b) the flexible solar panel, c) the protective tubing protecting the electric leads, and d) the encased KEH device

4. FIELD EXPERIMENTS

Several field experiments with a single Western Finn cattle (Talvikki – born 2021) were performed in the spring and summer of 2023 at the Ahlman dairy farm to verify the functional operation of the designed wearable. The device was first tested in the facility's barn to ensure appropriate fitting and see how the cow reacts to it. After the fitting grazing experiments were conducted next taking place from 8:30 am to 3:30 pm and they were performed with two different KEH cavities and magnet sizes and they initially included the solar panel as well. The collar is fitted on the cow in the barn before the herd would walk out to the field (Figure 12 a) and it was taken off when upon their return to the barn.

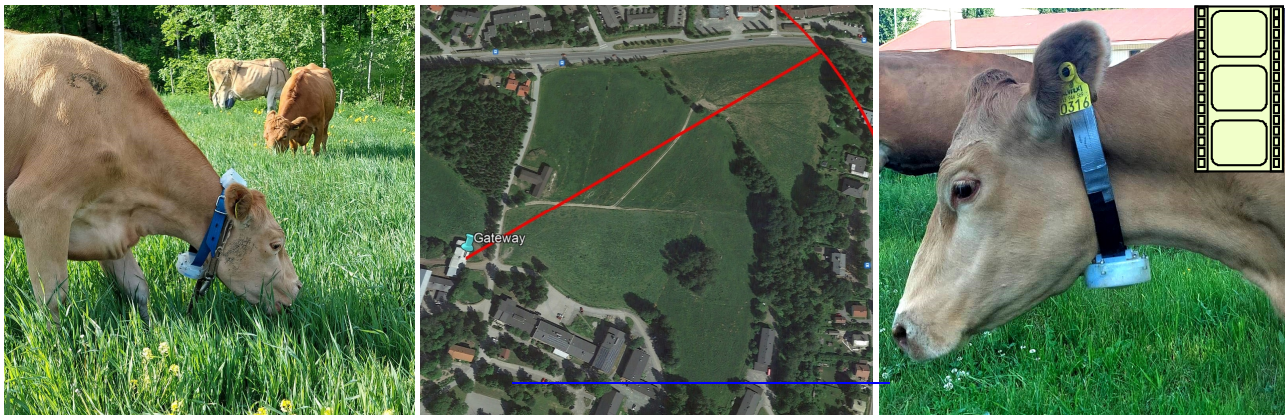

a) b) c)

Figure 12. a) image showing Talvikki grazing in the field equipped with the prototype collar, b) satellite image showing the diameter of the furthest transmission distance from the field to the gateway (420 m) and c) Video 1: Talvikki equipped with a prototype collar moving and grazing on the field. http://dx.doi.org/10.1117/12.3010124.1

A total of ten single day grazing experiments were performed: a) one experiment with the Version 1 KEH device combined with the solar panel, b) eight experiments with Version 1 KEH device with the solar panel taped off, and c) one experiment with the Version 2 KEH device and the solar taped off. The Ahlman dairy farm fields are divided into different paddocks. The cows are taken to different paddocks each day. The gateway is placed in a barn nearby the field. The distance from the very end of the furthest section of the field to the gateway is approximately 420 meters. A satellite image of the Ahlman dairy farm fields depicting the furthest possible distance to the gateway can be seen in Figure 12 b). Temperature samples, message reception time stamps, RSSI and the number of received messages from the wearable are logged on the gateway by means of a microSD card. The memory card is removed from the gateway after each experiment and the data is downloaded and analysed on a PC. Figure 12 c) contains a link to a video showing how the cow moved and grazed uninhibited with the attached collar.

By measuring the power consumption of one full cycle of the wearable's operation (Section 3.2) and by knowing the number of received messages logged on the SD card in the gateway, we can estimate total electrical energy converted from the energy of animal locomotion by means of the employed version of the KEH device. This estimate does not result with the total amount of harvested energy, but the amount of harvested energy that was successfully utilized by the MCU (meaning most probably more energy is produced than accounted for). A certain number of messages was certainly lost due to due to packet loss caused by terrain irregularities and certain types of obstructions present on the fields thus reducing LoRa capabilities. From our experience the LoRa technology has in fact proven to be quite sensitive to many parameters surrounding the transmitter (vegetation, other cow's bodies etc.).

The KEH device should have enough mass for the collar to stay in the right position, where the KEH device stays at the bottom of the collar, under the cow's neck. The designed KEH device including the protective cover's mass is ~0.5 kg, which was found out to be heavy enough, but also light enough so the cow doesn't mind it. This mass corresponds to masses of regularly used cattle marking weights. The designed prototype is also sturdy enough to handle the harsh farm environment where it was observed in regular collisions with farm infrastructure, other cattle and in contact with drinking water. Another thing that must be considered is the MBM's pull force which shouldn't be so high that the MBM gets frequently stuck to farm infrastructure, e.g., farm gates or water tanks, or so strong that it picks up metal debris which cannot be shaken off by itself. The pulling forces of the used MBMs were observed to be in the correct practical range.

4.1 Field experiment results

In the initial field test, we utilized both the solar panel and Version 1 KEH device in a multi-modal energy harvesting system. During this experiment we recorded more than 3000 transmissions thus proving that the solar panel works. Due to impossibility to distinguish between the amounts of energy from the solar panel and Version 1 harvester, the solar panel was taped off in the following eight experiments which were used only to validate the functionality of the KEH device. In those experiments we had to overcome certain difficulties like message reception optimization (for lower power from KEH), antenna type and position optimization (for both the collar and the gateway), and collar fit optimization (a tighter fit). The last three consecutive experiments with Version 1 harvester, lasting for ~7 hours each are shown in Figure 13 where a) displays the number of successfully received transmissions logged by the gateway, b) shows the total amount of energy produced by the Version 1 harvester, and c) shows the measured temperature of the cow's body. The amount of energy in joules presented in Figure 13 is calculated by multiplying the number of transmissions received by the gateway with the amount of electric energy needed by the wearable to run a one full cycle consisting of start-up/measurement/data transmission. Due to possibly unreceived and obstructed LoRa transmissions the amount of energy is speculatively larger than the one presented in the graphs.

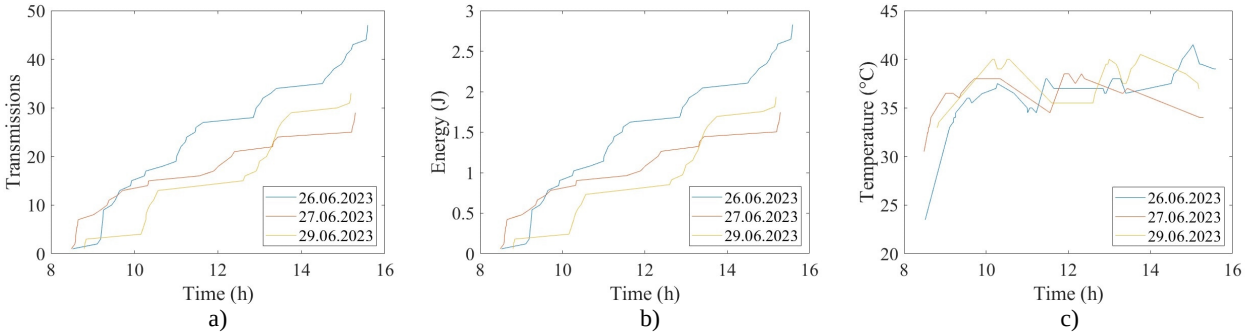

a) b) c)

Figure 13. Graphs showing results obtained with the KEH device Version 1 during three separate days: a) number of transmissions reaching the gateway, b) calculated harvested total energy, and c) cow's skin temperature graph. The time presented in the graphs is real time 8 AM – 16 AM

Upon exiting the barn at ~08:30 AM and arriving on the designated grazing paddock, a period of intense activity occurs where the herd moves around the paddock and commences grazing. A significant amount of kinetic energy can be expected to be harvested from this period. This is easily seen in Figure 13 a) and b) where around 08:30 – 09:00 AM there is a sharp rise in the number of transmissions and the amount of calculated produced energy. Usually, ~2 hours after the first period of intensive movement and grazing cows lay down, rest, and ruminate. At this point, the amount of harvested energy is expected to drop, and this can again be observed in the parts of Figure 13 a) and b) where the flat part of the graphs indicate idling time. It's interesting to note that even at this period the harvester can harvest small amounts of locomotion energy and still transmit one or two messages to the gateway. These grazing/idling cycles then repeat until it's time for the cattle to head back to the barn (15:30 PM). In total, during the three experiments, the Version 1 KEH device produced 1.8 – 2.8 J of energy while successfully transmitting 4 to 7 messages per hour to the gateway.

Finally, Version 2 of the KEH device was attached to the collar and a field grazing experiment was undertaken again to see how the increased dimensions of the KEH device would influence the amount of generated power. In this experiment the Version 2 KEH device harvested triple the amounts of energy when compared to Version 1 which resulted in three times as much transmitted messages while keeping the total volume of the device relatively similar as seen in Figure 14 a) and b) and summarized in Table 3. The temperature measurements performed to establish this benchmark system are far from ideal. We've learned it's difficult to obtain correct body temperature measurements by using a contact digital thermometer which can be observed from both Figure 13 c) and Figure 14 c). Even though the measured values of temperatures are in the cattle body temperature ranges (cattle core temperature is ~38 °C [54]), the oscillations due to outside temperature are too big to make it a reliable way of measuring body temperature. For this study the temperature sensor was used as a realistic sensing load for the benchmark system while obtaining the correct temperatures wasn't the main objective.

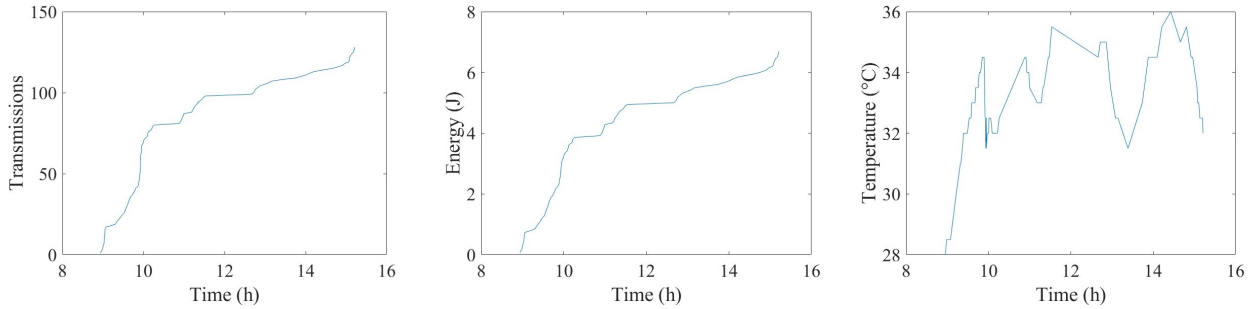

a) b) c)

Figure 14. Graphs showing the result obtained with the KEH device Version 2: a) number of transmissions reaching the gateway, b) calculated harvested total energy and c) cow's skin temperature graph

During the experiment with the device Version 2, an accelerometer was attached to the casing of the KEH device and interfaced to an acceleration and voltage logger as shown in Figure 7 and explained in Section 3.2. This was done so that the charging cycles of the capacitor could be logged together with the 3-D acceleration of the KEH device casing when inertially excited by the cow's locomotion as shown in Figure 15. If compared with the data from Figure 15 a), it can be clearly noticed that the number of transmitted messages and the amount of produced energy correlates beautifully with the activity level monitored on the KEH device casing with clearly pronounced activity/idling time periods. It's interesting to observe from Figure 15 b) how well this 3-D KEH spherical design couples with the animal's locomotion. Even during the cycles of evident idling/ruminating the KEH device is harvesting energy from the slightest of movements and charging the capacitor constantly. To further confirm this, Figure 15 c) presents a detail of the capacitor's logged voltage level shown concurrently with the logged acceleration levels in a 6 minute window. Here we can observe distinct separate PMIC charging cycles of the capacitor associated with low acceleration levels produced by the animal (< 1 *g*).

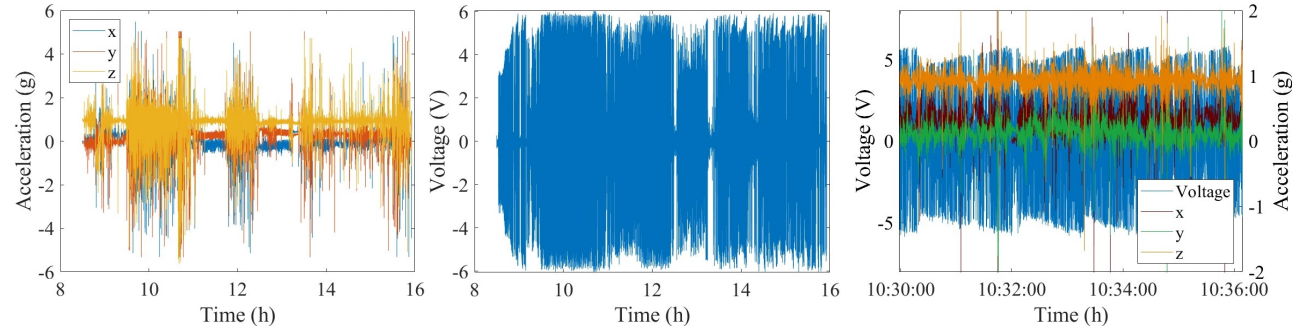

a) b) c)

Figure 15. Results from concurrent measurement of the capacitor voltage and acceleration levels of the casing during the ~7 h experiment with Version 2: a) acceleration logged on the KEH device casing, b) capacitor voltage level, and c) a detail of a) and b) parts showing distinct cycles of the capacitor charging together with the acceleration used as a source of energy.

5. CONCLUSIONS AND OUTLOOK

This paper details the development of an experimentally optimized and field validated 3-D electromagnetic KEH device intended for smart farming wearable applications – especially with grazing animals like cattle, sheep, goats and pigs. In the presented case a spherical KEH generator with a MBM is analysed, optimized and field tested on live cattle. The empirical optimization procedure was used to identify the optimal diameter of the pickup coil and the number of turns. A pendulum analogy was used to find the damping period of the harvesting device and to modify the spherical casing's diameter to match the intended cattle locomotion frequency. A complete smart farming benchmarking system was built and tested – first in the lab and then in the field. The system consisted of a kinetically powered cattle collar with a wireless body temperature sensor and a gateway device installed onsite used to log the sensor data. The collar consisted of a KEH generator, solar panel and complete control electronics: a PMIC, MCU, LoRa radio, and a digital contact temperature sensor for measuring cattle body temperature. Two versions of the KEH device were built – one optimized for size and the other slightly larger optimized for more power. Both were tested in a series of field experiments with a

single cow. At first the wearable was tested in multi-modal power generation where solar and kinetic energy were harvested in parallel. After proving the multi-modality in operation, the solar panel was taped off and the experiments continued focusing only on KEH device functionality. Both versions of the KEH device proved able to power the intended application and run from 5 to 20 complete cycles per hour where the usual cycle consists of MCU start-up / measurement / transmission and uses ~40 mJ of energy (Table 3).

Table 3. Comparison of results obtained with two versions of the optimized KEH device: Volume indicates only the volume of the harvester (spherical cavity) while the mass includes the mass of the harvester and the protective casing.

KEH device experiment	Transmissions per hour	Energy accumulation rate (J/h)	Volume (cm^3)	Mass (kg)
Version 1 (average)	5.4	0.3	290	0.450
Version 2	20.4	1.1	346	0.5

Further optimization is necessary to determine if the possible use of a tethering magnet would facilitate stronger and more efficient induction if the MBM is kept approximately orientated upon reaching low points of the cavity. Additionally, the device volume could be optimized so that certain degrees of freedom are limited based on cattle locomotion measurements – in a way enabling the MBM to move only in the direction of strongest excitation. The MBM is very susceptible to slightest of cattle locomotion and can produce energy using very low excitation levels (< 1 *g)* which leads to an another interesting application for the developed device. Because the MBM movement correlates extremely well to animal activity levels the KEH device can also be used as an inductive activity sensor akin to an accelerometer and in this way serve a double purpose.

6. ACKNOWLEDGEMENTS

This project received funding from the Business Finland - Research2Business funding framework (project nr. 2140/31/2023). The authors would like to thank the Materials science and environmental engineering group and the Innovation services of Tampere University and Ahlmanin koulun Säätiö for their assistance with this work.

REFERENCES

[1] Jawad, H. M. et al., “Energy-Efficient Wireless Sensor Networks for Precision Agriculture: A Review”, Sensors (17), 1781 (2017).
[2] Bahr, C. et al., [EIP-AGRI Focus Group: Precision Farming - final report], European Commission, 4-6 (2015).
[3] Ali, A. et al., “Recent progress in energy harvesting systems for wearable technology”, Energy Strategy Reviews (49), 101124 (2023).
[4] Sezer, N. and Koç, M., “A comprehensive review on the state-of-the-art of piezoelectric energy harvesting”, Nano Energy (80), 105567 (2021).
[5] Nozariasbmarz, A. et al., “Review of wearable thermoelectric energy harvesting: From body temperature to electronic systems”, Applied Energy (258), 114069 (2020).
[6] Gawron, P. et al., “A Review on Kinetic Energy Harvesting with Focus on 3D Printed Electromagnetic Vibration Harvesters”, Energies (14), 6961 (2021).
[7] Munirathinam, P. et al., “A comprehensive review on triboelectric nanogenerators based on Real-Time applications in energy harvesting and Self-Powered sensing”, Materials Science and Engineering: B (297), 116762 (2023).
[8] Harerimana, F. et al., “Efficient circuit design for low power energy harvesting”, AIP Advances (10), 105006 (2020).
[9] Watkins, R., [The origins of self-winding watches 1773 – 1779], Self-published, Richard Watkins, (2016).
[10] Bogoff, S., “Perrelet Self-Winding”, Bogoff.com, <https://www.bogoff.com/pocket/8219.html> (05 February 2024).
[11] Sequent AG, <https://sequentworld.com/en-fr> (05 February 2024).
[12] Matrix Industries, <https://www.powerwatch.com/> (05 February 2024).
[13] Paci, P. et al., “Designing for wearability: an animal-centred framework”, Proc. of the Sixth International Conference on Animal-Computer Interaction, 1–12 (2019).

[14] Morrone, S., et al., “Industry 4.0 and Precision Livestock Farming (PLF): An up to Date Overview across Animal Productions”, Sensors (22), 4319 (2022).
[15] Aquilani, C., et al., “Review: Precision Livestock Farming technologies in pasture-based livestock systems”, Animal (16)1, 100429 (2022).
[16] Zhang M., et al., ”Wearable Internet of Things enabled precision livestock farming in smart farms: A review of technical solutions for precise perception, biocompatibility, and sustainability monitoring”, Journal of Cleaner Production (312), 127712 (2021).
[17] Tzanidakis, C., et al., “Precision Livestock Farming Applications (PLF) for Grazing Animals”, Agriculture (13), 288 (2023).
[18] Golinski, P., et al., ”Virtual Fencing Technology for Cattle Management in the Pasture Feeding System—A Review”, Agriculture (13), 91 (2023).
[19] Ma D., et al., ”Sensing, Computing, and Communications for Energy Harvesting IoTs: A Survey”, IEEE Communications Surveys & Tutorials (22)2, 1222-1250 (2020).
[20] Chen Y., et al., "A Survey on LPWAN-5G Integration: Main Challenges and Potential Solutions," IEEE Access (10), 32132-32149 (2022).
[21] Zhang, P., et al., “Hardware design experiences in ZebraNet”, Proc. of the 2nd international conference on Embedded networked sensor systems - SenSys ’04, 227 (2004).
[22] Bruce T., et al., “Development of a datalogger for assessment of solar energy harvesting in submarine environments,” Proc of IEEE Oceans '17 Conference Anchorage -Alaska, 1–9, (2017).
[23] Goldsmith, W. M., et al., “Performance of a low-cost, solar-powered pop-up satellite archival tag for assessing post-release mortality of Atlantic bluefin tuna (Thunnus thynnus) caught in the US east coast light-tackle recreational fishery”, Anim. Biotelemetry (5)1, 29 (2017).
[24] Loreti P., et al., “The design of an energy harvesting wireless sensor node for tracking pink iguanas,” Sensors, (19)5, 1–16 (2019).
[25] Mansfield, K. L., et al., “Satellite tag attachment methods for tracking neonate sea turtles,” Marine Ecology Progress Series (457), 181–192 (2012).
[26] Anderson, D. M., “Virtual fencing – past, present and future “, The Rangeland Journal (29), 65–78 (2007).
[27] Bäumker, E., et al., “A Fully Featured Thermal Energy Harvesting Tracker for Wildlife”, Energies (14), 6363 (2021).
[28] Aktakka, E. E., et al., “Energy scavenging from insect flight”, Journal of Micromechanics Microengineering (21)9, 095016 (2011).
[29] Reissman, T., et al., “Electrical power generation from insect flight,” Proc. of SPIE Smart Structures and Materials+ Nondestructive Evaluation and Health Monitoring (7977), 797702 (2011).
[30] Shafer, M. W., et al., “A Practical Power Maximization Design Guide for Piezoelectric Energy Harvesters Inspired by Avian Bio-Loggers,” Proc. of ASME 2012 Conference on Smart Materials, Adaptive Structures and Intelligent Systems (2), 819-828 (2013).
[31] Badr, B. M., et al., “Design of a Low Frequency Piezoelectric Energy Harvester for Rodent Telemetry,” Ferroelectrics (481)1, 98–118 (2015).
[32] Häsler, E., et al., “Implantable physiological power supply with PVDF film”, Ferroelectrics (60)1, 277–282 (1984).
[33] Dagdeviren, C., et al., “Conformal piezoelectric energy harvesting and storage from motions of the heart, lung, and diaphragm,” Proc. of the National Academy of Sciences (111),1927-1932 (2014).
[34] Li, H., et al., “An Energy Harvesting Underwater Acoustic Transmitter for Aquatic Animals,” Scientific Reports (6)1, 33804 (2016).
[35] Reuter, T., et al., “Test of a generator in the rumen of cattle for energy harvesting to biosensors,” Biomedical Engineering (57), 572–575, 2012.
[36] Noda, T., et al. “Harvesting energy from the oscillation of aquatic animals: testing a vibration-powered generator for bio-logging data logger systems,” Journal of Advanced Marine Science and Technology Society (20)1–2, 37–43 (2014).
[37] Gutierrez, A., et al., “Cattle-powered node experience in a heterogeneous network for localization of herds,” IEEE Transactions on Industrial Electronics (60)8, 3176–3184 (2013).
[38] Blazevic, D., et al., “Kinetic energy harvesting potential of grazing livestock” Proc. of European Conference on Precision Livestock Farming 22' (10), 1054-1062 (2022).

[39] Blazevic, D., et al., “A farm animal kinetic energy harvesting device for IoT applications”, Proc. of SPIE Energy Harvesting and Storage: Materials, Devices, and Applications XII. (12090), 1209005 (2022).
[40] Gregersen, T., et al., “A novel kinetic energy harvesting system for lifetime deployments of wildlife trackers”, PLoS ONE (18) 5, e0285930 (2023).
[41] Tang, L., et al., “Broadband Vibration Energy Harvesting Techniques” In: Elvin, N., Erturk, A. (eds), Advances in Energy Harvesting Methods, (2013).
[42] Bowers, B. J. and Arnold, D. P., “Spherical, rolling magnet generators for passive energy harvesting from human motion”, Journal of Micromechanics and Microengineering (19), 094008 (2009).
[43] Moss, S. D., et al., “Hybrid rotary-translational vibration energy harvester using cycloidal motion as a mechanical amplifier”, Applied Physics Letters (104), 033506 (2014).
[44] Inman, D. J., [Engineering vibration, 4th ed.], Prentice-Hall, Upper Saddle River, N.J., (2014).
[45] Schmickl, S,. et al., “Microwatt power management: challenges of on-chip energy harvesting”, Elektrotechnik & Informationtechnik (138), 31-36 (2021).
[46] LinearTechnology, LTC3588-1 Nanopower Energy Harvesting Power Supply – Datasheet, 2015
[47] Analog Devices, Ultralow Power Energy Harvester PMUs with MPPT and Charge Management ADP5091/ADP5092, Datasheet, 2017
[48] Bhawiyuga, A., et al., “LoRa-MQTT gateway device for supporting sensor-to-cloud data transmission in smart aquaculture IoT application,” Proc. of the International conference on sustainable information engineering and technology (SIET), IEEE, 187–190 (2019).
[49] DS18B20 – Programmable Resolution 1-Wire Digital Thermometer, Datasheet, 2019
[50] Adafruit Feather M0 Adalogger, Website: (accessed on 6.7.2023) https://www.adafruit.com/product/2796
[51] Adafruit RFM69HCW and RFM9X LoRa Packet Radio Breakouts. Website: (accessed on 6.7.2023) https://learn.adafruit.com/adafruit-rfm69hcw-and-rfm96-rfm95-rfm98-lora-packet-padio-breakouts/overview
[52] DS3231, Extremely Accurate I2C-Integrated RTC/TCXO/Crystal, Datasheet, 2015
[53] Xtrinsic MMA8451Q 3-Axis, 14-bit/8-bit Digital Accelerometer, Datasheet, 2013
[54] Godyń, D., et al., “Measurements of peripheral and deep body temperature in cattle – A review”, Journal of Thermal Biology (79), 42-49 (2019).